J. Fluid Mech. (1988), *vol.* 187, *pp.* 45–59
Printed in Great Britain

The mechanisms underlying flow-induced instabilities of cylinder arrays in crossflow

By M. P. PAÏDOUSSIS AND S. J. PRICE
Department of Mechanical Engineering, McGill University, Montreal, Québec, H3A 2K6 Canada

(Received 24 March 1987)

This paper aims to shed some light on the physical mechanisms involved in flow-induced instabilities of arrays of cylinders in crossflow. In the framework of quasi-steady fluid-dynamic theory, two distinct mechanisms are discussed. The first is similar but not identical to that associated with classical galloping; i.e. it is a negative fluid-dynamic damping mechanism and may obtain even if a single cylinder in the array is free to oscillate with only one degree of freedom. Unlike classical galloping, it is intimately related to the time delay experienced in the wake structure, and hence the fluid forces, adjusting to displacements of the cylinder. The second mechanism is similar to wake flutter; i.e. it is controlled by non-conservative fluid-dynamic stiffness effects and generally requires relative motion between adjacent cylinders in the array, although there is no reason why it should not occur for a single flexible cylinder with two degrees of freedom. The two mechanisms generally coexist, but each is predominant over different ranges of system parameters.

1. Introduction

Arrays of cylinders in various regular geometric configurations and subject to crossflow are commonly found in a variety of industrial equipment; e.g. in heat exchangers, steam generators, boilers and condensers. It is well known that in addition to turbulent buffeting and resonance with wake-related Strouhal-type periodicities in the interstitial flow, such arrays are subject to a flow-induced oscillatory instability at sufficiently high flow velocities (Païdoussis 1980, 1981, 1983), commonly referred to as fluidelastic instability. The amplitudes associated with the resultant limit-cycle motion are typically large enough to cause inter-cylinder clashing and damage to the equipment. It is not surprising, therefore, that, from the 1960s on, considerable effort has been devoted to establishing means for predicting the critical flow velocity for this instability.

There exist today several semi-empirical and quasi-analytical theories for predicting the onset of fluidelastic instabilities: namely, by Roberts (1966), Connors (1970) and Blevins (1974, 1977*a*, *b*), Tanaka & Takahara (1981) and Chen (1983*a*, *b*), Lever & Weaver (1982, 1986*a*, *b*), Païdoussis *et al.* (1984, 1985), and Price & Païdoussis (1984, 1986*a*, *b*). Discussion of these theories, as well as classifications of the theories in different ways, can be found in recent work by Chen (1987) and Païdoussis (1987).

Obviously, in each theoretical model a more or less clear explanation is given of the various elements of the fluid-dynamic forces incorporated in the analysis; sometimes, an assessment is also provided of their relative importance in precipitating the instability. Thus, of particular significance to the present work is the finding (Chen

1983*a*, *b*; Price & Païdoussis 1984) that fluidelastic instability is controlled (i) by negative fluid-dynamic damping forces for low values of the mass-damping parameter $\bar{m}\delta$, where $\bar{m} = m/\rho D^2$, m being the cylinder mass per unit length and D its diameter, δ the *in vacuo* logarithmic decrement of damping and ρ the fluid density, and (ii) by fluid-dynamic 'stiffness' terms, i.e. by a displacement-controlled mechanism, for large values of $\bar{m}\delta$.

Nevertheless, what is missing is a relatively simple and clear physical explanation as to what are exactly the fluid-dynamical mechanisms causing fluidelastic instability, beyond the general statement that they are related to negative damping and/or non-conservative displacement-dependent fluid-dynamic forces. Also missing is a discussion of the relationship between this instability and other, long established and better understood phenomena in aero/hydroelasticity, such as galloping, for instance. The purpose of this paper is to attempt to do just that. For convenience and ease of interpretation of the results, this will be done in the context of quasi-steady fluid-dynamic theory.

2. Modified quasi-steady theory

Consider an array of cylinders, a portion of which is shown in figure 1 (*a*), subjected to crossflow. For simplicity, consider for the moment that all the cylinders are rigid, except one, which is flexibly mounted and motions of which are characterized by the displacements x and y.

Then, assuming no mechanical coupling between motion in the x- and y-direction, the equation of motion of the cylinder in the y-direction may be written as

$$ml\ddot{y} + c\dot{y} + ky = F_y, \tag{1}$$

where F_y is the fluid-dynamic force, l the length of the cylinder, and c and k are the effective mechanical damping and stiffness of the cylinder, respectively.

According to quasi-steady (or quasi-static) theory the forces acting on the oscillating cylinder are approximately the same as the static forces at each point of the cycle of oscillation, provided that the approach velocity is properly adjusted to take into account the velocity of the cylinder, in the manner shown in figure 1 (*b*). Thus, F_y may be written as

$$F_y = \tfrac{1}{2}\rho U_r^2 lD\{C_\mathrm{L}\cos(-\alpha) - C_\mathrm{D}\sin(-\alpha)\}, \tag{2}$$

where U_r and α are defined in figure 1 (*b*) and given by

$$U_r = [(U-\dot{x})^2 + \dot{y}^2]^{\frac{1}{2}}, \quad -\alpha = \sin^{-1}(\dot{y}/U_r);\dagger$$

C_L and C_D are the static lift and drag coefficient, respectively, which for small motions about the equilibrium position may be expressed in linearized form as

$$C_\mathrm{L} = C_{\mathrm{L}_0} + \left(\frac{\partial C_\mathrm{L}}{\partial x}\right)x + \left(\frac{\partial C_\mathrm{L}}{\partial y}\right)y,$$

and similarly for C_D. Then, (2) may be linearized to give

$$F_y = \tfrac{1}{2}\rho U^2 lD\left[-2C_{\mathrm{L}_0}\left(\frac{\dot{x}}{U}\right) + \left(\frac{\partial C_\mathrm{L}}{\partial x}\right)x + \left(\frac{\partial C_\mathrm{L}}{\partial y}\right)y - C_{\mathrm{D}_0}\left(\frac{\dot{y}}{U}\right)\right]. \tag{3}$$

† This peculiar definition of α is for the sake of consistency with Den Hartog's (1932, 1956), which is useful when the two analyses are compared later on.

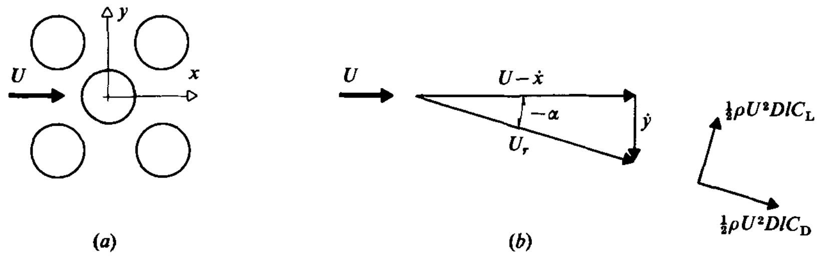

FIGURE 1. (*a*) Cross-sectional view of a small part of an array of cylinders in crossflow; (*b*) velocity vector diagram.

For a regular symmetric geometrical pattern of the cylinders, such as shown in figure 1(*a*), $C_{L_0} = 0$ and $\partial C_L/\partial x = 0$. Hence, (3) simplifies to

$$F_y = \tfrac{1}{2}\rho U^2 lD\left[\left(\frac{\partial C_L}{\partial y}\right)y - C_{D_0}\left(\frac{\dot{y}}{U}\right)\right]. \tag{4}$$

The discussion so far has been in terms of traditional quasi-steady fluid-dynamics. It is known, however, that there is a time-lag between cylinder displacement and the fluid-dynamic forces generated thereby. This may be thought to be related to the delay in the two fluid streams on either side of the cylinder readjusting to the changing configuration as the cylinder oscillates (Lever & Weaver 1982); alternatively, it may be thought to be associated with the retardation that the fluid experiences as it nears the cylinder, notably in the vicinity of a stagnation point, in conjunction with inter-cylinder positions having meanwhile changed as a result of cylinder motions (Simpson & Flower 1977; Price & Païdoussis 1984, 1986*a*, *b*). Perhaps this time-lag may most easily be conceived as a delay in the viscous wake adjusting continuously to the changing conditions imposed by the vibrating cylinder (Païdoussis, Mavriplis & Price 1984). As a first approximation, this time-delay, τ, may be expressed as

$$\tau = \mu D/U, \tag{5}$$

where $\mu \sim O(1)$ (Price & Païdoussis 1984).† Hence, taking this effect into account, and assuming harmonic motions, such that $y = y_0 \exp(i\omega t)$, equation (4) may be written as

$$F_y = \tfrac{1}{2}\rho U^2 lD\left[e^{-i\omega\tau}\left(\frac{\partial C_L}{\partial y}\right)y - C_{D_0}\left(\frac{\dot{y}}{U}\right)\right]. \tag{6}$$

3. The negative damping mechanism

Equations (1) and (6) may be combined and re-written in the form

$$\ddot{y} + \left[\left(\frac{\delta}{\pi}\right)\omega_0 + \frac{1}{2}\left(\frac{\rho UD}{m}\right)C_{D_0}\right]\dot{y} + \left[\omega_0^2 - \frac{1}{2}\left(\frac{\rho U^2 D}{m}\right)\left(\frac{\partial C_L}{\partial y}\right)e^{-i\omega\tau}\right]y = 0, \tag{7}$$

where ω_0 is the radian natural frequency of the cylinder and δ its logarithmic

† This is an elementary approximation, as compared to those in more highly developed areas of fluid-elasticity, e.g. unsteady fluid dynamics and stall flutter of aerofoils (Bisplinghoff, Ashley & Halfman 1955; Ericsson & Reding 1988). It should be remembered, however, that when bluff bodies are involved the fluid dynamics is considerably more difficult to deal with than for aerofoils.

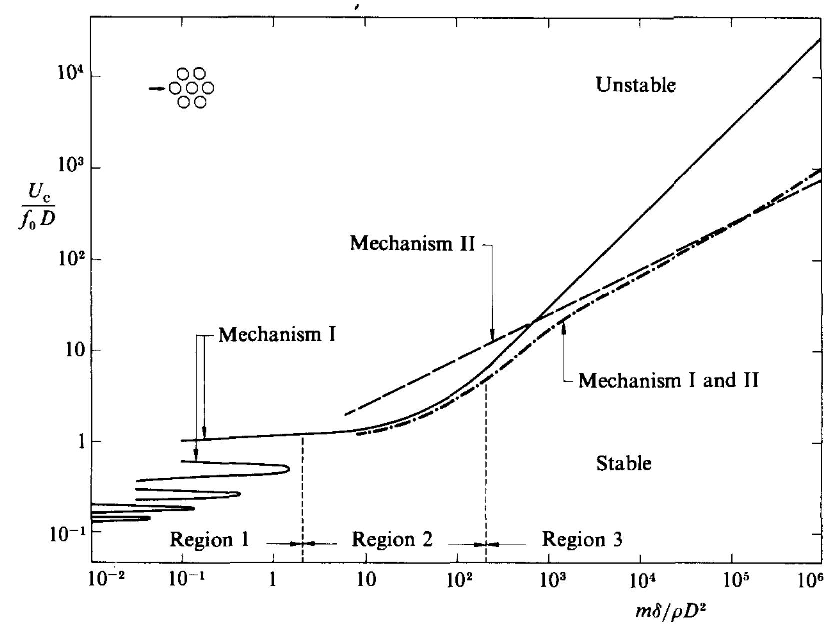

FIGURE 2. Stability diagram for a rotated triangular array with pitch-to-diameter ratio 1.375 (see elemental part of the array on the upper left-hand corner). Mechanism I refers to the negative-damping one-degree-of-freedom mechanism (§3); mechanism II refers to the two-degree-of-freedom 'wake-flutter' mechanism (§§5 and 7). Region 1 is where $U/\omega D$ is small enough for $\sin(\omega D/U) \neq \omega D/U$; region 2 is where $\sin(\omega D/U) \approx \omega D/U$; region 3, for larger $U/\omega D$, is where both mechanisms I and II contribute to the instability.

decrement (both in vacuum). For harmonic motions, utilizing (5), the total damping term is found to be proportional to

$$\left[\left(\frac{\delta}{\pi}\right)\omega_0\,\omega+\frac{1}{2}\left(\frac{\rho U D}{m}\right)\omega C_{D_0}+\frac{1}{2}\left(\frac{\rho U^2 D}{m}\right)\left(\frac{\partial C_L}{\partial y}\right)\sin\left(\frac{\mu\omega D}{U}\right)\right]. \tag{8}$$

Clearly, if the total damping becomes negative, then oscillations will be amplified; i.e. an oscillatory instability will arise. At the threshold of instability, say at $U = U_c$, the total damping will be zero.

If $U/\mu\omega D$ is sufficiently large ($\mu\omega D/U$ small) for the sine to be approximated by its argument, then setting expression (8) to zero yields

$$\frac{U_c}{f_0 D}=\left\{\frac{4}{-C_{D_0}-\mu D(\partial C_L/\partial y)}\right\}\frac{m\delta}{\rho D^2}, \tag{9}$$

where $f_0 = \omega_0/2\pi$. For obvious reasons, it is implicitly assumed that $U_c > 0$ and, hence, fluidelastic instability will occur provided that

$$-C_{D_0}-\mu D(\partial C_L/\partial y) > 0; \tag{10}$$

since $C_{D_0} > 0$ generally, this implies that instability will arise only provided that $\partial C_L/\partial y$ be sufficiently large and negative – which does in fact occur for many cylinder arrays, but not for all (Price & Païdoussis 1986*b*). Solutions given by relation (9) are shown in region 2 of figure 2.

It is important to notice the similarity of relation (10) to Den Hartog's (1932, 1956) criterion for galloping of iced overhead electrical conductors. In its original form this is given by

$$C_{D_0} + \frac{\partial C_L}{\partial \alpha} < 0; \tag{11}$$

however, if a time delay between conductor motion and lift force, of the same form as (5), is accounted for, then the Den Hartog criterion may be re-written as

$$C_{D_0} + \mathrm{Re}\,[e^{-i\omega\tau}\,\partial C_L/\partial\alpha] < 0. \tag{12}$$

Of course, in classical quasi-steady theory, $\tau = 0$ and thus (11) and (12) are identical.

Now, if y is expressed as a function of α, namely $y = -(U/i\omega)\,\alpha$, then $\partial C_L/\partial\alpha$ may be re-written as $-(U/i\omega)(\partial C_L/\partial y)$; so, assuming $\omega\tau$ to be small and τ to be given by (5), inequality (12) may be expressed as

$$C_{D_0} + \mu D(\partial C_L/\partial y) < 0,$$

which is exactly the same as inequality (10).

Several important insights may be gained by consideration of relations (9) and (10), as follows.

(i) It is obvious that if there were no time delay, i.e. $\mu = 0$, no oscillatory fluidelastic instability could arise. This agrees with the results obtained previously by Price & Païdoussis (1984, 1986*b*) and Païdoussis *et al.* (1984).† It is also true in Lever & Weaver's theory (1982, 1986*a*, *b*), although not explicitly stated. The only possible form of instability in such a case would be a static divergence (Païdoussis *et al.* 1984), which will be discussed in §4.‡

(ii) For small values of $U/\omega D$, the approximation of the sine function by its argument is no longer valid; setting the transcendental expression (8) to zero admits an infinite set of solutions for neutral stability, as the sine oscillates between -1 and 1. Some of the solutions represent the threshold from stability to instability, and some the reverse. Thus this leads to a spectrum of stable and unstable zones as $U/f_0 D$ is increased, as obtained by Lever & Weaver (1982, 1986*a*, *b*), Chen (1983*a*, *b*) and Price & Païdoussis (1984, 1986*a*, *b*). It is of interest that in such cases instabilities may arise not only for $\partial C_L/\partial y$ negative, but also positive and large. Typical solutions from the full form of expression (8) are presented in region 1 of figure 2.

(iii) The threshold of instability according to the approximations leading to (9) is insensitive to the frequency of oscillation in the fluid medium concerned, ω, depending only on the *in vacuo* frequency, ω_0 (and hence f_0) – something that has perplexed researchers in the past (see discussion by Païdoussis 1980, 1983 for example).

† Price & Païdoussis's (1984, 1986*b*) analytical models show that one-degree-of-freedom flutter is dependent on the existence of a time delay between cylinder motions and fluid-dynamic forces generated thereby. As the present work represents a simplification of these models towards facilitating an understanding of the nature of fluidelastic instability, it is not surprising that there is agreement with the present work in this crucial aspect. Païdoussis *et al.*'s (1984) analytical model is fundamentally different, in that all fluid-dynamic forces are derived by potential flow theory, ignoring the existence of wakes; significantly, oscillatory instabilities are predicted to occur only when a phase lag between cylinder motions and fluid-dynamic forces is heuristically introduced (to account for viscous, wake-related effects, as mentioned earlier).

‡ Of course, all statements made in (i) apply only to cylinders of circular cross-section, where the lift coefficient does not vary with the angle of attack.

(iv) The foregoing discussion is associated with y-direction motions. Proceeding in a similar manner for x-direction motions, it is found that for small $\omega D/U$,

$$\frac{U_c}{f_0 D} = \left\{\frac{4}{-2C_{D_0} - \mu D(\partial C_D/\partial x)}\right\} \frac{m\delta}{\rho D^2}, \tag{13}$$

so that for instability

$$-2C_{D_0} - \mu D(\partial C_D/\partial x) > 0 \tag{14}$$

must be satisfied. Although $\partial C_D/\partial x < 0$ often arises in several array configurations (Price & Païdoussis 1986*b*), it is generally smaller in magnitude than $|\partial C_L/\partial y|$, implying that the threshold of instability is more likely to be associated with y-direction motions, as observed experimentally. For larger $\omega D/U$, as for y-direction motions, multiple zones of instability may arise; furthermore, the instability may also be associated with $\partial C_D/\partial x$ positive and large.

(v) According to relationships (9) and (13), $U_c/f_0 D$ is proportional to $m\delta/\rho D^2$, or $\bar{m}\delta$. This appears to be correct in terms of experimental observations, in the middle range of $\bar{m}\delta$ (region 2 of figure 2). For sufficiently high $\bar{m}\delta$, however, characteristic of gaseous flows, experimental evidence suggests that either $U_c/f_0 D \propto (\bar{m}\delta)^{\frac{1}{2}}$ or $\propto \bar{m}^a \delta^b$, where $a \neq b$ and $a, b \leqslant \frac{1}{2}$, but certainly not $\propto \bar{m}\delta$. This is related to the increasing importance of the second mechanism associated with fluidelastic instability, to be discussed in §5.

4. Divergence instability

Examining (7), it may be verified that a single flexible cylinder in the array may become unstable by divergence (non-oscillatory static instability) if the stiffness term vanishes, which occurs, for $\omega D/U$ sufficiently small, at $U = U_{cd}$ given by

$$\frac{U_{cd}}{fD} = \left\{\frac{8\pi^2}{D(\partial C_L/\partial y)}\right\}^{\frac{1}{2}} \left\{\frac{m}{\rho D^2}\right\}^{\frac{1}{2}} \tag{15}$$

in the y-direction;† similarly for the x-direction, with $\partial C_D/\partial x$ replacing $\partial C_L/\partial y$. This implies that for divergence, either $\partial C_L/\partial y$ or $\partial C_D/\partial x$ must be positive, which is opposite to the normal requirement for oscillatory instability. Hence, arrays subject to the usual, oscillatory fluidelastic instability will not be prone to divergence. As most types of cylinder arrays are subject to oscillatory fluidelastic instability, it is perhaps not surprising that no experimental observation of divergence has ever been reported. However, very recently and evidently for the first time, divergence has been observed by the authors and co-workers in a rotated square array with pitch-to-diameter ratio of 1.5 – and is reported here for the first time. Significantly, this array was found to be resistant to the normal, oscillatory fluidelastic instability, at least for a single flexible cylinder in the array (Price & Païdoussis 1986*b*).

The mechanism of divergence is the same as that of buckling of a column subjected to axial load; if, when the column is flexed, the load-related lateral force exceeds the flexural restoring force, then the system behaves as if it had a negative net stiffness. For the problem at hand, writing $\omega_0^2 = k_{eff}/m$, the restoring force is clearly

† This expression is really independent of the mass of the cylinder, as may easily be verified and as it should be. The way it is written, however, in terms of the 'standard' non-dimensional groups, makes it appear otherwise.

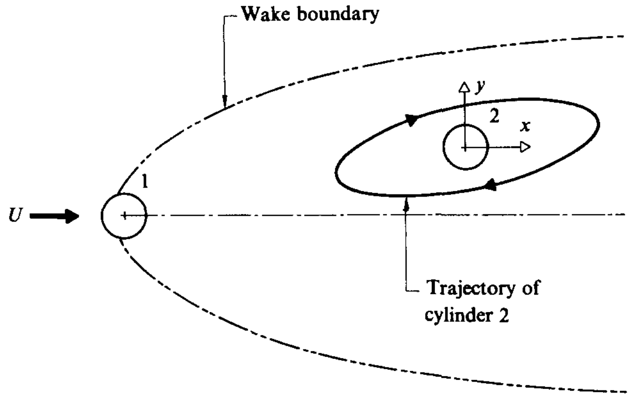

FIGURE 3. Wake flutter of a leeward electrical conductor in the wake of another, showing a typical trajectory during flutter.

proportional to $k_{\text{eff}}\,y$, while the lift-related force (for $\cos\omega\tau \approx 1$) is proportional to $\frac{1}{2}\rho U^2 lD(\partial C_L/\partial y)\,y$; hence, if $\partial C_L/\partial y$ is positive, i.e. if the lift increases with lateral displacement, then, for sufficiently large U, the latter term will become larger than the restoring term, precipitating divergence.

5. The wake-flutter mechanism

This mechanism has been studied extensively in connection with instabilities of bundles (or clusters) of overhead transmission lines (typically involving two or four wires) subjected to transverse wind, commonly referred to as sub-span oscillations (Simpson 1971; Price 1975; Simpson & Flower 1977).

Suppose that a leeward conductor undergoes an oval motion, as shown in figure 3, in the wake of a windward conductor. The flow-field being viscous and hence the force field on the moving conductor non-conservative, energy may be gained from the fluid, or lost to it, in the course of a cycle of motion. In the former case, the oscillatory motion will be amplified; i.e. an instability will arise. This mechanism, in its 'stripped down' form is purely a displacement-dependent or stiffness-controlled mechanism, in contrast to that of §3, which is predominantly a velocity-dependent (or negative damping) mechanism.

A characteristic of this mechanism is that at least two degrees of freedom must be involved in the motion (in the foregoing example, motions in the x- and y-direction of one conductor); alternatively (and more typically for cylinder arrays), motions of adjacent cylinders in either direction may be involved.

To appreciate how this instability arises, an elementary system of two flexible cylinders will be considered. Although the system has four degrees of freedom, the mathematical model to be considered will only have two. This is because it has been shown previously (Price & Païdoussis 1984) that, at the onset of instability, motions are predominantly in one direction (in the x-direction for a double row of flexible cylinders, and in the y-direction if this same double row is part of a larger, otherwise rigid array of cylinders); similarly, in the case of overhead transmission lines, it is often assumed that only the leeward conductor is free to oscillate (in both the x- and y-direction). Hence, two degrees of freedom are sufficient to capture the essential physical features of the instability. Thus, the coupled equations of motion of the system may be written as follows:

$$([\boldsymbol{M}]+[\boldsymbol{M}]_{\mathrm{f}})\{\ddot{z}\}+([\boldsymbol{C}]+[\boldsymbol{C}]_{\mathrm{f}})\{\dot{z}\}+([\boldsymbol{K}]+[\boldsymbol{K}]_{\mathrm{f}})\{z\}=\{\boldsymbol{0}\}, \tag{16}$$

where the unsubscripted matrices are associated with the mechanical system and those with suffix f are associated with the fluid-dynamic terms; $\{z\}$ is the displacement vector, so that for motion of two cylinders in the y-direction, for instance, $\{z\}=\{y_1,y_2\}^{\mathrm{T}}$.

Concerning the mechanical system itself, the following set of demonstrably reasonable and, for heat exchanger arrays, realistic assumptions are made: the modal masses, as well as the mechanical and damping terms, are equal in the two degrees of freedom concerned; also, there is no mechanical coupling between the two degrees of freedom. Thus, $M_{11}=M_{22}=ml$; $C_{11}=C_{22}=c$; $K_{11}=K_{22}=k$; and all off-diagonal terms in the mechanical matrices are zero.

Concerning the fluid-dynamic matrices, a set of, at first sight, more tenuous assumptions are made, which are nevertheless justifiable *a posteriori*, some by numerical computations, as will be discussed in the next paragraph: (i) the flow retardation (time-delay) terms are entirely removed; (ii) the virtual (added) mass terms are neglected; (iii) the fluid-dynamic damping terms are neglected, as compared to the mechanical damping terms. Thus, (16) is simplified to

$$\begin{bmatrix} ml & 0 \\ 0 & ml \end{bmatrix}\{\ddot{z}\}+\begin{bmatrix} c & 0 \\ 0 & c \end{bmatrix}\{\dot{z}\}+\begin{bmatrix} k & 0 \\ 0 & k \end{bmatrix}\{z\}+\tfrac{1}{2}\rho U^2 lD\begin{bmatrix} \kappa_{11} & \kappa_{12} \\ \kappa_{21} & \kappa_{22} \end{bmatrix}\{z\}=\{\boldsymbol{0}\}, \tag{17}$$

where z is either x or y, and the κ_{ij} are of the form $-\partial C_{\mathrm{F}}/\partial z_j$, in which C_{F} stands for either C_{D} or C_{L} accordingly to whether $z=x$ or y.

The removal of the flow retardation terms ($\mu=0$) ensures that the generator of the negative-damping mechanism discussed in §3 is removed, so that instability, if it can arise at all, will have to be due to some other mechanism. Assumption (ii) above is justified partly for simplicity and partly because the mechanism under discussion is dominant for gaseous flows, where virtual mass effects are negligible. The ratio of the fluid-dynamic to the mechanical damping terms (with flow retardation removed) may be shown to be $(C_{\mathrm{D}_0}/4\bar{m}\delta)(fD/U)$ and $(C_{\mathrm{D}_0}/2\bar{m}\delta)(fD/U)$, respectively for motions in the y- and x-direction (Price & Païdoussis 1984, 1986*a*). Clearly, if instability occurs at sufficiently large values of U/fD, these ratios become small, typically 1/40 and 1/20, respectively, and the fluid-dynamic damping may be neglected; hence assumption (iii) is justified.

Let us now consider the dynamical implications of the form of the simplified equation of motion (17). Introducing the notation $\eta=z/D$, $\bar{t}=\omega_0 t$, the equation of motion may be written in dimensionless form as follows:

$$\begin{bmatrix} 1 & 0 \\ 0 & 1 \end{bmatrix}\begin{Bmatrix} \eta_1'' \\ \eta_2'' \end{Bmatrix}+\frac{\delta}{\pi}\begin{bmatrix} 1 & 0 \\ 0 & 1 \end{bmatrix}\begin{Bmatrix} \eta_1' \\ \eta_2' \end{Bmatrix}+\begin{bmatrix} 1 & 0 \\ 0 & 1 \end{bmatrix}\begin{Bmatrix} \eta_1 \\ \eta_2 \end{Bmatrix}+\frac{\bar{U}^2}{2\bar{m}}\begin{bmatrix} \bar{\kappa}_{11} & \bar{\kappa}_{12} \\ \bar{\kappa}_{21} & \bar{\kappa}_{22} \end{bmatrix}\begin{Bmatrix} \eta_1 \\ \eta_2 \end{Bmatrix}=\{0\}, \tag{18}$$

where $\bar{U}=U/\omega_0 D$, $\bar{m}=m/\rho D^2$, $\bar{\kappa}_{ij}=D\kappa_{ij}$ and $(\;)'=\mathrm{d}/\mathrm{d}\bar{t}$.

Assuming harmonic solutions of the form $\boldsymbol{\eta}=\boldsymbol{\eta}_0\exp(\lambda\bar{t})$, the characteristic equation is given by

$$\lambda^4+\left[\frac{2\delta}{\pi}\right]\lambda^3+\left[2+\left(\frac{\delta}{\pi}\right)^2+\left(\frac{\bar{U}^2}{2\bar{m}}\right)(\bar{\kappa}_{11}+\bar{\kappa}_{22})\right]\lambda^2$$

$$+\left[\left(\frac{\delta}{\pi}\right)\left\{2+\left(\frac{\bar{U}^2}{2\bar{m}}\right)(\bar{\kappa}_{11}+\bar{\kappa}_{22})\right\}\right]\lambda+\left[1+\left(\frac{\bar{U}^2}{2\bar{m}}\right)(\bar{\kappa}_{11}+\bar{\kappa}_{22})+\left(\frac{\bar{U}^2}{2\bar{m}}\right)^2(\bar{\kappa}_{11}\bar{\kappa}_{22}-\bar{\kappa}_{12}\bar{\kappa}_{21})\right]=0.$$

The condition of zero total damping, i.e. the boundary of an oscillatory instability, may be obtained by application of the Routh criterion, or

$$p_1 p_2 p_3 - p_4 p_1^2 - p_0 p_3^2 = 0,$$

where the p_i are the coefficients of λ^i. This leads to the following quadratic expression for $\bar{U}^2/2\bar{m}$:

$$\left(\frac{\bar{U}^2}{2\bar{m}}\right)^2 [(\bar{\kappa}_{11}-\bar{\kappa}_{22})^2+4\bar{\kappa}_{12}\bar{\kappa}_{21}]+2\left(\frac{\bar{U}^2}{2\bar{m}}\right)\left[\left(\frac{\delta}{\pi}\right)^2(\bar{\kappa}_{11}+\bar{\kappa}_{22})\right]+4\left(\frac{\delta}{\pi}\right)^2 = 0. \tag{19}$$

In general, the solution to this equation is cumbersome, but, if $(2\pi/\delta)[(\bar{\kappa}_{11}-\bar{\kappa}_{22})^2+4\bar{\kappa}_{12}\bar{\kappa}_{21}]^{\frac{1}{2}}/(\bar{\kappa}_{11}+\bar{\kappa}_{22})$ is sufficiently small compared with unity (which is the case for small enough δ), then an approximate solution of relatively simple form may be obtained, i.e.

$$\bar{U}_c \approx \left\{\frac{-16/\pi^2}{(\bar{\kappa}_{11}-\bar{\kappa}_{22})^2+4\bar{\kappa}_{12}\bar{\kappa}_{21}}\right\}^{\frac{1}{4}} (\bar{m}\delta)^{\frac{1}{2}}, \tag{20a}$$

where it was assumed that a real $\bar{U}_c$ exists; in more conventional terms, this equation may be written as

$$\frac{U_c}{f_0 D} = \left\{\frac{-256/\pi^2}{(\bar{\kappa}_{11}-\bar{\kappa}_{22})^2+4\bar{\kappa}_{12}\bar{\kappa}_{21}}\right\}^{\frac{1}{4}} \left(\frac{m\delta}{\rho D^2}\right)^{\frac{1}{2}}. \tag{20b}$$

Furthermore, for cylinders deep enough in the array (i.e. away from the first or last few rows) $\bar{\kappa}_{11} = \bar{\kappa}_{22}$, and equation (20*b*) may be simplified further to

$$\frac{U_c}{f_0 D} = \left\{\frac{-64\pi^2}{\bar{\kappa}_{12}\bar{\kappa}_{21}}\right\}^{\frac{1}{4}} \left(\frac{m\delta}{\rho D^2}\right)^{\frac{1}{2}}. \tag{20c}$$

Despite the simplifying assumptions leading to equation (20*c*), it does give results in excellent agreement with those obtained from the complete set of equations, as discussed in §§6 and 7. Three important conclusions may be drawn directly from equations (20):

(i) for instability to occur, the stiffness matrix should not only be asymmetric ($\bar{\kappa}_{12} \neq \bar{\kappa}_{21}$), but the signs of the off-diagonal terms must be opposite;

(ii) the dependence of $U_c/f_0 D$ on the mass-damping parameter is that of a square-root relationship, rather than a linear one as was the case for the one-degree-of-freedom negative-damping mechanism discussed in §3;

(iii) if the diagonal terms $\bar{\kappa}_{11}$ and $\bar{\kappa}_{22}$ are unequal, this leads to an increase of $U_c/f_0 D$.

The requirement in (i) above is often met in practice. Thus, for a so-called rotated triangular array with pitch-to-diameter ratio $p/D = 1.375$ (see figure 4), measurements have given $\bar{\kappa}_{12} = -D(\partial C_{L_1}/\partial y_2) = 16.7$ and $\bar{\kappa}_{21} = -D(\partial C_{L_2}/\partial y_1) = -26.6$, where cylinder 1 is in one row and cylinder 2 is diagonally adjacent to it in the row immediately upstream, as shown in figure 4.

Physically, the non-equality of $\bar{\kappa}_{12}$ and $\bar{\kappa}_{21}$ is an attribute of the non-conservativeness of the system. Thus, if instead of fluid-dynamic coupling there were mechanical coupling involving springs, then the forces could be derived from a potential function and clearly $k_{12} = k_{21}$ would have been obtained: the force on cylinder 1 due to motion of cylinder 2 is equal to the force on cylinder 2 due to motion of cylinder 1, in the same directions. This is the well-known reciprocity principle in solid mechanics. Significantly, if the flow field is modelled as a purely potential flow (Païdoussis *et al.* 1984) then the fluid-dynamic stiffness matrix obtained analytically

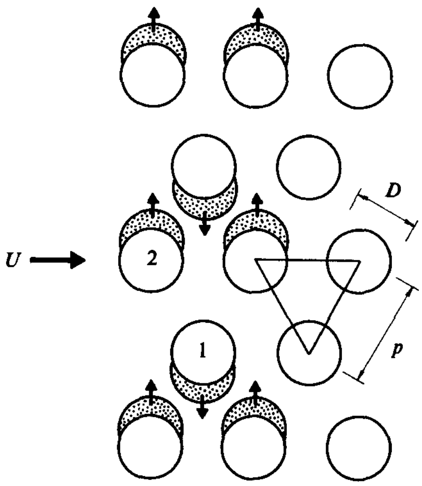

FIGURE 4. Part of a rotated triangular array, showing representative cylinders 1 and 2, as well as the pattern of motion during flutter; motions in adjacent rows are 90° out of phase.

is symmetric and, hence, the instability cannot materialize. In reality, of course, the flow-field is rotational with separated viscous flow regions (the existence of the wakes cannot be overlooked), and it is because of this that $\bar{\kappa}_{12} \neq \bar{\kappa}_{21}$ and, indeed, that $\bar{\kappa}_{12}\bar{\kappa}_{21} < 0$.

Another attribute of the viscous, rotational nature of the flow field and the non-conservativeness (asymmetry) of the stiffness matrix is that the energy derived from the flow is path-dependent; i.e. the phase in the motions of the two cylinders is of importance, as in Connors' (1970) mechanism, which is fundamentally the same as that described above. Indeed, comparing equations (20*b*, *c*) to Connors' expression, $U_c/f_0 D = K(m\delta/\rho D^2)^{\frac{1}{2}}$, where K is an experimentally determined constant, the similarity becomes self-evident. Also, the expression obtained by Blevins (1977*b*), who generalized Connors' model, is in fact identical to the simplified expression derived here, equation (20*c*), although the notations differ. Nevertheless, it is believed that in the development presented here the assumptions made are justified more clearly, and hence the limitations involved are delineated more systematically; moreover, this mechanism is considered in a unified manner, together with the negative-damping one-degree-of-freedom mechanism presented in §3, which is not considered at all in the Connors–Blevins work.

6. Dependence of the wake-flutter mechanism on mechanical damping

An apparent paradox in the results obtained for the wake-flutter mechanism is that the critical flow velocity is proportional to the square-root of the logarithmic decrement of mechanical damping, δ. This contrasts to the results normally obtained for classical coupled-mode flutter instabilities, where the effect of mechanical damping is so insignificant, that it is usually ignored; see for example Bisplinghoff, Ashley & Halfman (1955) for the flutter analysis of aircraft wings, and Simpson (1971), Price (1975) and Price & Piperni (1986) for analyses of overhead transmission bundles.

To resolve this paradox it should first be realized that in the aforementioned classical aeroelastic analyses, the two modes, associated with the two degrees of

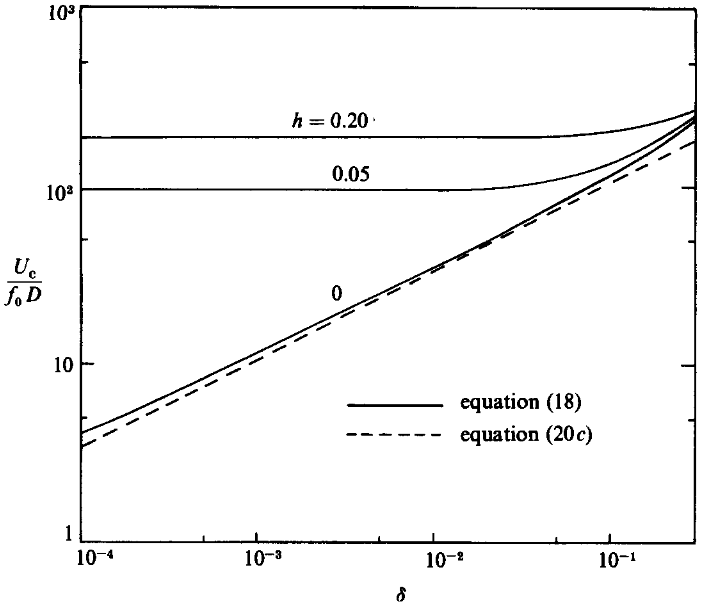

FIGURE 5. The effect of differences in the *in-vacuo* modal stiffnesses, h, in the two-degree-of-freedom system of §§5 and 6 on the functional relationship between $U_c/f_0 D$ and δ. Rotated triangular array (pitch-to-diameter ratio $p/D = 1.375$, $\bar{m} = 10^5$).

freedom involved, have distinct (non-equal) natural frequencies under 'wind-off' (or *in vacuo*) conditions. Thus, the mechanical stiffness matrix in (17) may in this case be written as

$$\begin{bmatrix} 1 & 0 \\ 0 & 1+h \end{bmatrix}, \tag{21}$$

where h represents the difference in modal stiffness in the two degrees of freedom. The second point to realize is that even small values of h can have a profound effect on the relationship between $U_c/f_0 D$ and δ, as will presently be shown.

Consider the same rotated triangular array, associated with figures 2 and 4. Solutions of (17), but with the mechanical stiffness as given by (21), were obtained for various values of h and are shown in figure 5. It is seen that for $h = 0$, i.e. when the two modes have equal frequency, $U_c/f_0 D$ is sensibly proportional to $\delta^{\frac{1}{2}}$, and the solution is very closely approximated by (20*c*). However, even for $h = 0.05$, which corresponds to a 2.5 % difference in natural frequencies, the functional dependence of $U_c/f_0 D$ on δ is entirely different: for $\delta \leqslant 0.02$, $U_c/f_0 D$ is insensitive to δ. For $h = 0.2$, this effect extends to $\delta \leqslant 0.10$.

This resolves the apparent paradox referred to at the beginning of this section and, in this respect, reconciles the difference in dynamical behaviour of cylinder arrays and overhead transmission lines. However, it is also of direct interest to the dynamics of arrays, in heat exchangers for example, where in the so-called U-bend region there exist substantial differences in natural frequency of adjacent cylinders. It is important to be aware that this 'detuning' of adjacent cylinders leads to a considerable reduction in the efficacy of raising the threshold for fluidelastic instability by means of increased mechanical damping.

$m\delta/\rho D^2$	10^5	10^4	10^3	10^2
$U_c/f_0 D$ 'full solution'	236	70.4	17.3	2.91
$U_c/f_0 D$ 'simplified solution'	244	77.9	24.7	7.79

TABLE 1. Comparison between the critical flow velocities for fluidelastic instability obtained via (i) the full, constrained-mode solution and (ii) the simplified solution of (20) and (22), for a rotated triangular array with $p/D = 1.375$, and $\delta = 0.01$ throughout.

7. Wake-flutter stability boundaries for cylinder rows

Of course, the results of §5 may be applied directly by considering a system of two flexible cylinders in an array of otherwise rigid ones. Numerical results were obtained in this manner and were found to be similar to those to be discussed below, which were obtained by a generalization of the foregoing, whereby the results are more representative of the stability of a fully flexible array. This is done by considering an infinitely long double-row of flexible cylinders, within a larger array of rigid cylinders.

It is realized at the outset that, realistically, all the cylinders in the array are fluid-dynamically coupled in a chain-like manner, so that the correct choice of a two-cylinder 'kernel' representative of the array should take this fact into consideration, as well as the relative phase in the motions of cylinders in the same row; this leads to the so-called 'constrained-mode solution', as described by Price & Païdoussis (1986*a*), whereby the analysis of the two-cylinder kernel becomes representative of an infinite array of flexible cylinders. It is shown that this results (Price & Païdoussis 1986*a*) in

$$\bar{\kappa}_{12} = -D\left(\frac{\partial C_{L_1}}{\partial y_2}\right)(1+\delta_1), \quad \bar{\kappa}_{21} = -D\left(\frac{\partial C_{L_2}}{\partial y_1}\right)(1+\delta_2), \tag{22}$$

where the δ can take on the values of 1, 0 or -1; similarly if the $\bar{\kappa}$ involve C_D and x. If $\delta_1 = \delta_2 = 1$, this signifies that cylinders in the same row are presumed to move in phase; if they are equal to -1, then in antiphase. All possible δ are utilized and the minimum U/fD obtained thereby is considered to be the critical one; significantly, the same set of δ is found to give the best agreement with the full, unconstrained analysis of multi-degree-of-freedom long rows of flexible cylinders (Price & Païdoussis 1984). In the results to be presented in what follows, this is achieved with $\delta_1 = \delta_2 = 1$.

Solutions obtained by (18) and (22) are represented in region 3 of figure 2, marked as due to mechanism II. Of course, in general, both mechanisms I and II are at work, i.e. both the single-degree-of-freedom negative damping mechanism of §3 and the stiffness-controlled mechanism discussed here. The results obtained by the full solution of the equations of motion, without the introduction of the simplifications leading to (17), are also shown in region 3 of figure 2, marked as due to both mechanisms I and II.

The results shown in table 1 give numerical comparisons of the critical flow velocities obtained by the full constrained-mode solution of the equations of motion to the 'simplified solution' according to (20) and (22). It is clear that, for large values of $\bar{m}$ (and hence $\bar{m}\delta$), there is not much difference between the two; this signifies that the instability is predominantly due to the position-dependent 'wake-flutter' mechanism discussed here. As $\bar{m}$ is diminished, however, the differences become more pronounced, indicating the increasing contribution of the negative-damping one-degree-of-freedom mechanism (mechanism I) to the destabilization of the system.

The instability in table 1 involves y-direction motions (see figure 4), where motions in adjacent rows are 90° out of phase. If, instead, an array of only two rows is considered, then the instability is found to involve predominantly x-direction motions. Indeed, in principle, there is no *a priori* reason why wake-flutter instabilities in some arrays should not involve only one flexible cylinder in the array instead of two, the two requisite degrees of freedom being associated with x- and y-motions of the cylinder.

8. Conclusion

The foregoing work represents an attempt to elucidate the mechanisms underlying fluidelastic instability of cylinder arrays in crossflow, as well as providing links to the well-known classical galloping and two-degree-of-freedom wake-flutter mechanisms.

It is shown that, provided the mass-damping parameter $\bar{m}\delta$ is sufficiently small, the instability is a modified form of the galloping mechanism first proposed by Den Hartog for the observed limit-cycle motions of iced transmission lines. The essence of the difference between this 'classical' galloping and what occurs in cylinder arrays is that in the latter case the mechanism is intimately connected with a time delay, which is associated with the time taken for the wake flow to adjust to cylinder motions. Nevertheless, the mechanism is fundamentally similar to classical galloping, in that it involves but one degree of freedom and is associated with negative fluid-dynamic damping overcoming the positive mechanical damping of the cylinder. Thus, stability boundaries in this case may be obtained by considering motions of a single cylinder in the array in one direction, while adjacent cylinders are assumed to be immobile.

This is the mechanism of instability predominating in regions 1 and 2 of figure 2. Stability boundaries may be obtained by satisfying expression (8) set to zero for y-motions, or the equivalent one for x-motions. If $U/\omega D$ is sufficiently large, then stability boundaries may be obtained by the even simpler relations (9) or (10), or the equivalent ones for x-motions. This mechanism is the one recognized by Chen (1983*a*, *b*) and Price & Païdoussis (1984, 1986*a*, *b*) as the dominant mechanism of instability for sufficiently small $\bar{m}\delta$ and by Lever & Weaver (1982, 1986*a*, *b*) as exclusively operative irrespective of $\bar{m}\delta$.

The objective of this paper was to elucidate, rather than predict, the instability. In this respect, it should be stressed that setting expression (8) to zero is not sufficient for predicting instability, in that C_{D_0} and $\partial C_L/\partial y$ cannot at present be predicted analytically, but must rather be obtained empirically.

In the higher range of $\bar{m}\delta$, region 3 of figure 2, a second destabilizing mechanism comes into play; for sufficiently high $\bar{m}\delta$ this mechanism becomes predominant, while the foregoing one contributes less. This is a position-dependent, fluid-dynamic stiffness-controlled mechanism, similar to that of wake flutter, long known to be responsible for the so-called sub-span oscillations of bundled electrical transmission lines. This mechanism requires at least two degrees of freedom of a system, and has been demonstrated here in terms of y- or x-motions of two adjacent cylinders in the array. It is intimately related to the fluid-dynamic coupling between motions in these two degrees of freedom, which, because of the rotational and viscous nature of the flow-field, does not exhibit reciprocity, as would be the case if coupling were of a mechanical nature. In matrix notation the coupling manifests itself in non-zero off-diagonal fluid-dynamic terms, which are not equal because of the non-conservativeness of the flow-field and hence of the system as a whole.

Based on a set of reasonable assumptions, the problem was simplified and it was possible to obtain simple relationships for the onset of instability according to this second mechanism, equations (20). It was found, *a posteriori* that these relationships are similar to that obtained previously by Connors (1970) and, in their simplest form, identical to that obtained by Blevins (1977*b*). The dominance of this mechanism for high $\bar{m}\delta$ was recognized in Chen's (1983*a*, *b*) and Price & Païdoussis's (1984, 1986*a*, *b*) work.

Significantly, the dependence of $U_c/f_0 D$ on $\bar{m}\delta$ is found to be different in different ranges of the latter parameter, as shown in figure 2, and in agreement with experimental observations (see Price & Païdoussis 1986*a*, *b*, for example). For low values of $\bar{m}\delta$ the principal instability boundary is insensitive to $\bar{m}\delta$ (region 1 of figure 2), although a set of secondary instability zones exists below that boundary. In the middle range of $\bar{m}\delta$, $U_c/f_0 D$ depends more or less linearly on that parameter (region 2). Finally, for sufficiently high $\bar{m}\delta$, $U_c/f_0 D$ depends on the square-root of $\bar{m}\delta$ (region 3), an attribute of the wake-flutter mechanism. These are of course generalizations; quantitatively, the extent of these three regions depends on the geometry of the array and, for regions 1 and 2, not only on the product $\bar{m}\delta$, but also on the specific values of $\bar{m}$ and δ – two independent dimensionless parameters which are only combined by convention and sometimes for convenience.

In some ways, the work in this paper is similar to Nakamura's (1978) attempt to classify and clarify the various types of wind-induced aeroelastic instabilities to which bridge decks may be subjected: notably, 'single degree of freedom (torsional) flutter', corresponding to the classical Den Hartog type galloping in this paper, and 'classical flutter' involving two interrelated degrees of freedom and corresponding here to wake flutter; as well as an 'intermediate type of flutter', where both mechanisms make a contribution. The authors are grateful to an anonymous referee for bringing this paper to their attention.

The authors gratefully acknowledge the support of the Natural Sciences and Engineering Research Council of Canada and Le Fonds FCAR (Formation des chercheurs et Aide à la recherche) of Québec.

REFERENCES

BISPLINGHOFF, R. L., ASHLEY, H. & HALFMAN, R. L. 1955 *Aeroelasticity*. Addison-Wesley.

BLEVINS, R. D. 1974 *Trans. ASME* J: *J. Pressure Vessel Tech.* **96**, 263.

BLEVINS, R. D. 1977*a* *Trans. ASME* I: *J. Fluids Engng* **99**, 457.

BLEVINS, R. D. 1977*b* *Flow-Induced Vibration*. Van Nostrand-Reinhold.

CHEN, S. S. 1983*a* *Trans. ASME J. Vib. Acoust. Stress & Reliab. Design* **105**, 51.

CHEN, S. S. 1983*b* *Trans. ASME J. Vib. Acoust. Stress & Reliab. Design* **105**, 253.

CHEN, S. S. 1987 *J. Fluids Struct.* **1**, 35.

CONNORS, H. J. 1970 In *Flow-Induced Vibration in Heat Exchangers* (ed. D. D. Reiff), p. 42. ASME.

DEN HARTOG, J. P. 1932 *Trans. AIEE* **51**, 1074.

DEN HARTOG, J. P. 1956 *Mechanical Vibrations*, 4th edn, §7.5. McGraw-Hill.

ERICSSON, L. E. & REDING, J. P. 1988 *J. Fluids Struct.* **2** (in the Press).

LEVER, J. H. & WEAVER, D. S. 1982 *Trans. ASME* J: *J. Pressure Vessel Tech.* **104**, 147.

LEVER, J. H. & WEAVER, D. S. 1986*a* *J. Sound Vib.* **107**, 375.

LEVER, J. H. & WEAVER, D. S. 1986*b* *J. Sound Vib.* **107**, 393.

NAKAMURA, Y. 1978 *J. Sound Vib.* **57**, 471.

PAÏDOUSSIS, M. P. 1980 In *Practical Experiences with Flow-Induced Vibrations* (ed. E. Naudascher & D. Rockwell), p. 1. Springer.

PAÏDOUSSIS, M. P. 1981 *J. Sound Vib.* **76**, 329.

PAÏDOUSSIS, M. P. 1983 *Nucl. Engng & Design* **74**, 31.

PAÏDOUSSIS, M. P. 1987 *Appl. Mech. Reviews* **40**, 163.

PAÏDOUSSIS, M. P., MAVRIPLIS, D. & PRICE, S. J. 1984 *J. Fluid Mech.* **146**, 227.

PAÏDOUSSIS, M. P., PRICE, S. J. & MAVRIPLIS, D. 1985 *Trans. ASME* I: *J. Fluids Engng* **107**, 500.

PRICE, S. J. 1975 *J. Sound Vib.* **38**, 125.

PRICE, S. J. & PAÏDOUSSIS, M. P. 1984 *J. Sound Vib.* **97**, 615.

PRICE, S. J. & PAÏDOUSSIS, M. P. 1986*a* *J. Sound Vib.* **105**, 121.

PRICE, S. J. & PAÏDOUSSIS, M. P. 1986*b* *Trans. ASME* I: *J. Fluids Engng* **108**, 193.

PRICE, S. J. & PIPERNI, P. 1986 In *Flow-Induced Vibration* (ed. S. S. Chen, J. C. Simonis & Y. S. Shin), p. 127, ASME. Also 1988 *J. Fluids Struct.* **2** (in the Press).

ROBERTS, B. W. 1966 *Mech. Engng Sci. Monograph* no. 4. I. Mech. E.

SIMPSON, A. 1971 *Aero. Q.* **23**, 101.

SIMPSON, A. & FLOWER, J. W. 1977 *J. Sound Vib.* **51**, 183.

TANAKA, H. & TAKAHARA, S. 1981 *J. Sound Vib.* **77**, 19.